Triadic balance and network evolution: Predictive modeling with signed networks–Supplementary Material

Hsuan-Wei Lee[1, 2*], Pei-Chin Lu[3], Hsiang-Chuan Sha[4], and Hsini Huang[5*]

1 Institute of Sociology, Academia Sinica, Taiwan
2 Department of Physics, National Taiwan University, Taiwan
3 Harris School of Public Policy, University of Chicago, United States
4 Virtual Science AI, United Kingdom
5 Institute of Public Administration, Leiden University, Netherlands

Corresponding authors: Hsuan-Wei Lee and Hsini Huang,
emails: waynelee1217@gmail.com, h.i.huang@fgga.leidenuniv.nl

A Appendix - Methods and Data

In this section, we outline the methods used to analyze the dynamic interactions within signed networks, leveraging principles from balance theory and advanced network modeling techniques. Our approach aims to capture nuanced relationships and predict future network formations accurately. Balance theory suggests that the relationships between any three nodes will eventually reach a balanced status, forming a triangle with an odd number of positive edges. For example, if nodes i and k are positively connected with a node j through edges (i, j) and (j, k), a positive tie will likely form between nodes i and k. This principle can be summarized as "the friend of my friend is my friend." To capture such relationships, we first define the notation used for the signed networks discussed herein. In this paper, at time t, P_{ij}^t represents the relationship between nodes i and j on the positive network, while N_{ij}^t represents their relationship in the negative network. We simultaneously consider two adjacency matrices, that is, P for the positive relationships and N for the negative relationships. Equation 1 provides a clear illustration of the notation.

$$\begin{cases} \mathbf{P}_{ij}^t = 1, & i \text{ has a positive tie with } j \text{ at time } t. \\ \mathbf{P}_{ij}^t = 0, & i \text{ has no positive tie with } j \text{ at time } t. \\ \mathbf{N}_{ij}^t = 1, & i \text{ has a negative tie with } j \text{ at time } t. \\ \mathbf{N}_{ij}^t = 0, & i \text{ has no negative tie with } j \text{ at time } t. \end{cases} \tag{1}$$

A.1 Dynamic Triadic Structures

This article focuses on the one-step change of the relations within a triple of vertices. Specifically, we distinguish between two types of dynamic triadic structures: triangle formation and triangle break. For triangle formation, we included all types of triadic structures that could form a triangle at time t but did not exist as a triangle at time $t-1$ (i.e., there were no ties, one tie, or two ties at time $t-1$). Conversely, for any three vertices forming a triangle at time $t-1$ but breaking out in t, the structure is defined as a triangle break. In Figure 1, we use `PForm` to illustrate how we define the one-step change to a triangle, considering transitions from 0 ties, 1 tie, and 2 ties.

As there are positive and negative networks, we distinguish the triadic behaviors on the single-layer network from the signed networks. On `PForm` and `PBrk`, we calculate the triangle formation and triangle break structures solely on the positive network and do not consider the node's behaviors on the negative network, `NForm` and `NBrk` vise versa. More specifically, for `PForm` and `PBrk`, we take a set of three nodes, say (i, j, k), arbitrarily and observe their behavior in the positive network from time $t-1$ to t. If the set of nodes forms a triadic closure, regardless of the direction, at time t from any non-triangle structure, then such three nodes are classified as "forming a triangle on the positive network." Conversely, when the node set (i, j, k) constitutes a triadic closure in time $t-1$ but breaks out at time t, then it is defined as "breaking a triangle in the positive network." When such triangle formation and break happens in the nega-

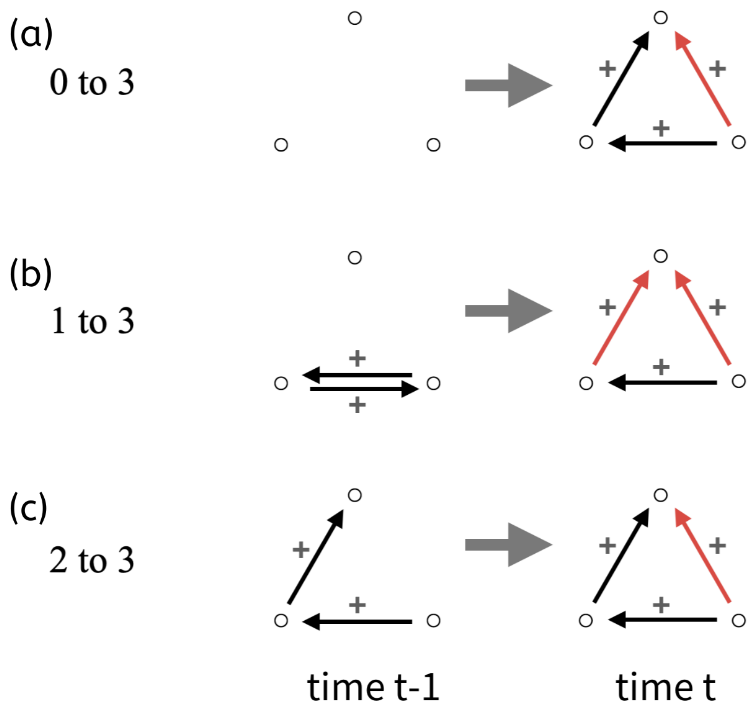

Figure 1: Examples of the definition of `PForm`

tive network, they are `NForm` or `NBrk`. The network structures above are classified as "single-layer triangle structures." As for `SFrom` and `SBrk`, "signed triangle structures," which collect the vertex's behavior across both positive and negative networks. Figure 2 shows some examples of temporal signed triangle structures. When counting the triangle form or break, we consider ties that are either in the positive or the negative network. To illustrate, if $P_{ij}^{t-1}, N_{jk}^{t-1}, P_{jk}^{t-1}$=(1,0,1) and $P_{ij}^{t}, N_{jk}^{t}, P_{jk}^{t}$=(1,1,1), then (i, j, k) are considered as composing an `SForm` structure. Equations 2 to 7 elaborate the definition of the six dynamic triangle structures we include in the models.

$$\texttt{PForm}_{ijk}^{t} = \Big[(\mathbf{P}_{ij}^{t-1} + \mathbf{P}_{ji}^{t-1} \leq 1) \bigcup ((\mathbf{P}_{ik}^{t-1} + \mathbf{P}_{ki}^{t-1} \leq 1) \bigcup ((\mathbf{P}_{jk}^{t-1} + \mathbf{P}_{kj}^{t-1} \leq 1)\Big] \bigcap \Big[(\mathbf{P}_{ij}^{t} + \mathbf{P}_{ji}^{t} \geq 1) \bigcap ((\mathbf{P}_{ik}^{t} + \mathbf{P}_{ki}^{t} \geq 1) \bigcap ((\mathbf{P}_{jk}^{t} + \mathbf{P}_{kj}^{t} \geq 1)\Big] \tag{2}$$

$$\texttt{PBrk}_{ijk}^{t} = \Big[(\mathbf{P}_{ij}^{t-1} + \mathbf{P}_{ji}^{t-1} \geq 1) \bigcap ((\mathbf{P}_{ik}^{t-1} + \mathbf{P}_{ki}^{t-1} \geq 1) \bigcap ((\mathbf{P}_{jk}^{t-1} + \mathbf{P}_{kj}^{t-1} \geq 1)\Big] \bigcap \Big[(\mathbf{P}_{ij}^{t} + \mathbf{P}_{ji}^{t} \leq 1) \bigcup ((\mathbf{P}_{ik}^{t} + \mathbf{P}_{ki}^{t} \leq 1) \bigcup ((\mathbf{P}_{jk}^{t} + \mathbf{P}_{kj}^{t} \leq 1)\Big] \tag{3}$$

$$\texttt{NForm}^t_{ijk} = \Big[(\mathbf{N}^{t-1}_{ij} + \mathbf{N}^{t-1}_{ji} \leq 1) \bigcup ((\mathbf{N}^{t-1}_{ik} + \mathbf{N}^{t-1}_{ki} \leq 1) \bigcup ((\mathbf{N}^{t-1}_{jk} + \mathbf{N}^{t-1}_{kj} \leq 1)\Big] \bigcap \Big[(\mathbf{N}^{t}_{ij} + \mathbf{N}^{t}_{ji} \geq 1) \bigcap ((\mathbf{N}^{t}_{ik} + \mathbf{N}^{t}_{ki} \geq 1) \bigcap ((\mathbf{N}^{t}_{jk} + \mathbf{N}^{t}_{kj} \geq 1)\Big] \tag{4}$$

$$\texttt{NBrk}^t_{ijk} = \Big[(\mathbf{N}^{t-1}_{ij} + \mathbf{N}^{t-1}_{ji} \geq 1) \bigcap ((\mathbf{N}^{t-1}_{ik} + \mathbf{N}^{t-1}_{ki} \geq 1) \bigcap ((\mathbf{N}^{t-1}_{jk} + \mathbf{N}^{t-1}_{kj} \geq 1)\Big] \bigcap \Big[(\mathbf{N}^{t}_{ij} + \mathbf{N}^{t}_{ji} \leq 1) \bigcup ((\mathbf{N}^{t}_{ik} + \mathbf{N}^{t}_{ki} \leq 1) \bigcup ((\mathbf{N}^{t}_{jk} + \mathbf{N}^{t}_{kj} \leq 1)\Big] \tag{5}$$

$$\texttt{SForm}^t_{ijk} = \Big[(\mathbf{P}^{t-1}_{ij} + \mathbf{P}^{t-1}_{ji} + \mathbf{N}^{t-1}_{ij} + \mathbf{N}^{t-1}_{ji} \leq 1) \bigcup ((\mathbf{P}^{t-1}_{ik} + \mathbf{P}^{t-1}_{ki} + \mathbf{N}^{t-1}_{ik} + \mathbf{N}^{t-1}_{ki} \leq 1) \bigcup (\mathbf{P}^{t-1}_{ik} + \mathbf{P}^{t-1}_{ki} + \mathbf{N}^{t-1}_{ik} \leq 1 + \mathbf{N}^{t-1}_{ki} \leq 1)\Big] \bigcap \Big[(\mathbf{P}^{t}_{ij} + \mathbf{P}^{t}_{ji} + \mathbf{N}^{t}_{ij} + \mathbf{N}^{t}_{ji} \geq 1) \bigcap (\mathbf{P}^{t}_{ik} + \mathbf{P}^{t}_{ki} + \mathbf{N}^{t}_{ik} + \mathbf{N}^{t}_{ki} \geq 1) \bigcap (\mathbf{P}^{t}_{jk} + \mathbf{P}^{t}_{kj} + \mathbf{N}^{t}_{jk} + \mathbf{N}^{t}_{jk} \geq 1)\Big] \tag{6}$$

$$\texttt{SBrk}^t_{ijk} = \Big[(\mathbf{P}^{t-1}_{ij} + \mathbf{P}^{t-1}_{ji} + \mathbf{N}^{t-1}_{ij} + \mathbf{N}^{t-1}_{ji} \geq 1) \bigcap ((\mathbf{P}^{t-1}_{ik} + \mathbf{P}^{t-1}_{ki} + \mathbf{N}^{t-1}_{ik} + \mathbf{N}^{t-1}_{ki} \geq 1) \bigcap (\mathbf{P}^{t-1}_{ik} + \mathbf{P}^{t-1}_{ki} + \mathbf{N}^{t-1}_{ik} \leq 1 + \mathbf{N}^{t-1}_{ki} \geq 1)\Big] \bigcap \Big[(\mathbf{P}^{t}_{ij} + \mathbf{P}^{t}_{ji} + \mathbf{N}^{t}_{ij} + \mathbf{N}^{t}_{ji} \leq 1) \bigcup (\mathbf{P}^{t}_{ik} + \mathbf{P}^{t}_{ki} + \mathbf{N}^{t}_{ik} + \mathbf{N}^{t}_{ki} \leq 1) \bigcup (\mathbf{P}^{t}_{jk} + \mathbf{P}^{t}_{kj} + \mathbf{N}^{t}_{jk} + \mathbf{N}^{t}_{jk} \leq 1)\Big] \tag{7}$$

A.2 Temporal ERGM in a Multilayer Network

In this study, we utilized statistical modeling techniques and analyses to investigate the research question. We employed baseline models to capture the initial dynamics of the networks, focusing on fundamental characteristics such as the number of edges and node degrees. We then expanded these models to incorporate indicators related to balance theory, examining their influence on network evolution. Furthermore, we extended our analysis to incorporate signed networks, treating them as multilayer networks comprising a positive and a negative layer. By transforming the multilayer networks into large monotonic networks, we employed the bootstrap TERGM (BTERGM) [4] to analyze the dynamic patterns of the longitudinal networks.

To represent the transformation, we constructed a large adjacency matrix of size $2n{\times}2n$, with the positive network positioned in the upper-right and the negative network in the lower-left. This reconstruction facilitated the application of multilayer

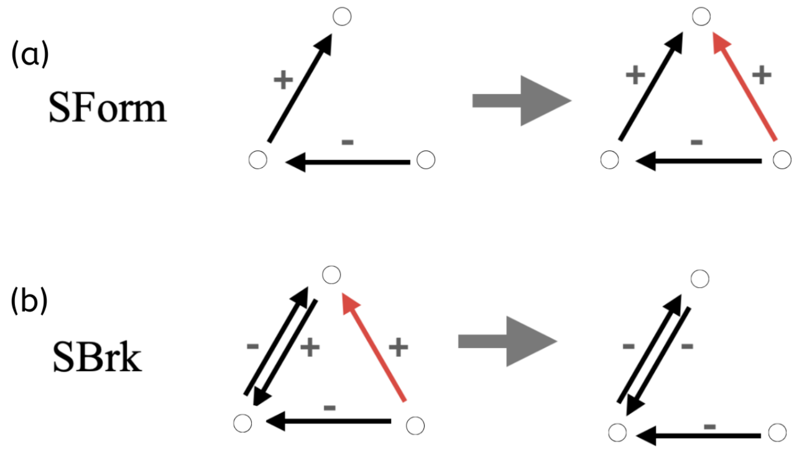

Figure 2: Examples of Temporal Signed Triangle Structures

modeling methods proposed [2]. Equation 8 illustrates the process of reconstructing the networks.

$$\begin{cases} \mathbf{X}_{ij}^{t} \subset \mathbf{P}_{ij}^{t}, & \text{if and only if } i, j \in [1, n] \text{ at time } t. \\ \mathbf{X}_{ij}^{t} \subset \mathbf{N}_{ij}^{t}, & \text{if and only if } i, j \in [n+1, 2n] \text{ at time } t. \end{cases} \tag{8}$$

In our analysis, we included dynamic triangle structures as edge covariates in the model and examined their effects on the network processes. This approach allowed us to investigate the interplay between triangle structures and other network characteristics within the context of the dynamic network modeling framework.

A.3 Network Characteristics and Data Collection

We adopt the method on three different signed networks, including two directed networks and one undirected network. The two directed networks are the Bitcoin trust network[1] and the Fraternity network[2]. In contrast, the undirected network is the Correlated of War (CoW) network[3]. The three networks vary in size, density, and positive-negative-tie ratio.

Table 1 shows the detailed information of the networks. The table presents network statistics for different datasets, with each data point representing the average value across multiple periods. The "Nodes" column denotes the average number of nodes in the network for each period. The "Edges (+,−)" column represents the average number of edges when the network is separated into positive and negative edges, providing insights into the average quantity of positive and negative connections in each period.

[1] The data are collected from Stanford Large Network Dataset Collection: https://snap.stanford.edu/data

[2] The data are collected from [1]

[3] The data are collected from [3]

Dataset	Nodes	Edges (+,−)	Edges (break, form)	Periods	Clustering coefficient	Directed network
Bitcoin Network	457.20	(202.56, 129.19)	(63.37, 49.09)	39	0.0937	Yes
Fraternity Network	9.5	(39.67, 48)	(115.43, 116.43)	15	0.6313	Yes
CoW Network	88.42	(40.31, 99.43)	(59.54, 167.44)	51	0.8855	No

Table 1: Statistics across the network evolution

However, the "Edges (break, form)" column indicates the average number of edges when the network is categorized into break and form edges, offering information on the average quantity of edges being formed or broken in each period. The "Periods" column denotes the total number of periods considered in the analysis for each respective network dataset.

A.4 Relabeling Process for Triangle Formation Analysis

We applied a 6-day moving average to the Bitcoin data, dividing it into daily slices. This transformation involved including all network ties within the time window of $[t-5, t]$ in period t of the adjusted network. Consequently, the transformed network exhibited increased density and a higher prevalence of triangle structures compared to the original network.

Notably, in the original Bitcoin network dataset, there were a total of 1,756 periods. However, when we split the network into positive and negative networks, we observed very few periods with the presence of triangles in the negative network. This posed a challenge as it hindered our ability to simulate the formation and dissolution of triangles in the model. Therefore, we decided to perform relabeling.

To illustrate this process, let us consider Figure 3 as an example. In the hypothetical scenario (not reflecting actual data), suppose the negative network only had triangles occurring in periods 100 to 105, 850 to 855, and 1,630 to 1,650. In the relabeling process, we would select periods 99 to 106, 849 to 856, and 1,629 to 1,651 instead. By including the preceding and succeeding periods of each interval, we capture the nature of triangle formations. For example, if a triangle appears in the 100th period but not in the 99th period, we can infer that a triangle formation occurs between the 99th and 100th periods. Based on the hypothetical scenario described above, a total of 39 periods would be selected for analysis. As certain models require the combination of both positive and negative networks, the relabeling process is also applied to the positive network, aligning its periods with those of the negative network. As a result of the relabeling process, the Bitcoin dataset used for analysis consisted of 39 periods.

For the Fraternity and CoW networks, the two other networks studied, we did not encounter the same challenge. Hence, the original number of periods was retained for these networks, with the Fraternity network spanning 15 periods and the CoW network spanning 51 periods.

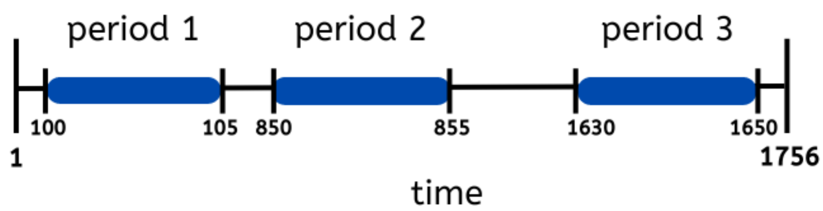

Figure 3: Illustrative Example: Relabeling Process and Period Selection

A.5 Model Types and Variable Classification

Our analysis began with a comprehensive exploration, estimating a total of 24 distinct models for each signed network. However, it is essential to clarify that these 24 models do not represent unique predictive models. Instead, they encompass various configurations, allowing for a comprehensive exploration of network dynamics. In reality, we have four fundamental models at the core of our analysis: the baseline model, the GWESP model (considering both positive and negative networks), the positive triangle model, and the signed triangle model. In addition to these models, we delved into the effects of balance theory by introducing variables that classified the networks into two categories: those that are consistent with the balance theory and those that are not. Specifically, we further categorized the already classified SForm and SBrk networks into SF-Bal, SB-Bal, SF-NBal, and SB-NBal. For instance, networks consistent with balance theory in SForm were classified as SF-Bal, while those inconsistent with balance theory were classified as SF-NBal. A similar classification was applied to SBrk networks.

To illustrate this further, let us consider Figure 4 as an example. In the first scenario, a positive connection is formed, but according to balance theory, a triangle with two positive edges and one negative edge is considered unstable and prone to break. Therefore, the first scenario is inconsistent with balance theory. Similarly, in the second scenario, a triangle with three negative edges is also considered unstable according to balance theory, leading to a classification as not consistent with balance theory. However, in the third and fourth scenarios, a triangle with one positive edge and two negative edges and a triangle with three positive edges can both exist stably, which is consistent with balance theory. Based on this logic, we further classify the originally categorized SForm and SBrk networks based on whether they are consistent with balance theory.

Table 2 provides an overview of the core model types considered in our analysis, including the baseline model, GWESP model, single-layer triangle model, and signed triangle model, along with their corresponding variables. Table 3 presents a comparison of the signed triangle model's performance in directed and modified undirected networks for both the Bitcoin and Fraternity networks. For example, in our study of network dynamics, a crucial aspect involves the classification of single-layer triangles, an operation that unveils intriguing insights into the underlying relationships within the network. This classification process serves as a cornerstone in comprehending the dynamics and behaviors exhibited by various entities within the network.

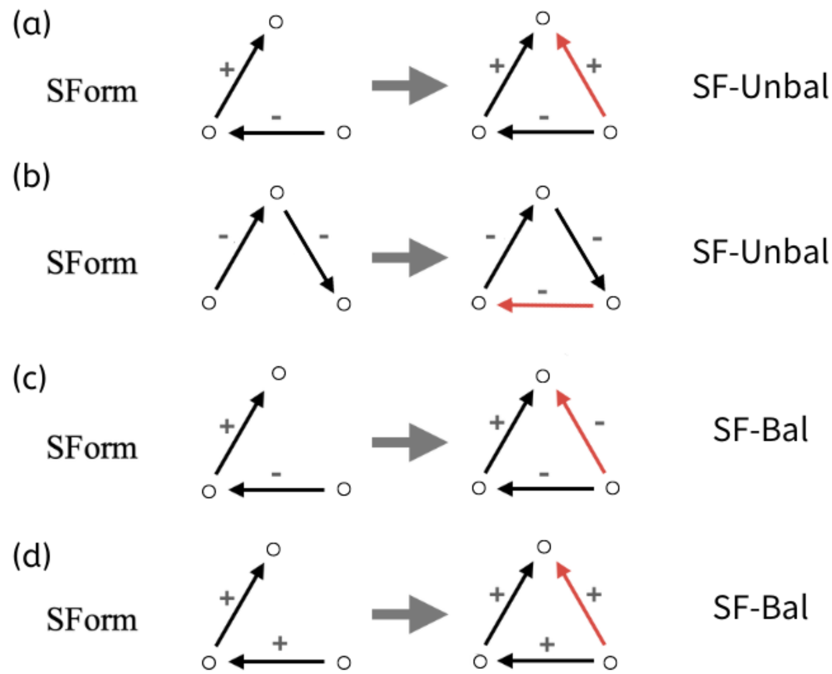

Figure 4: Illustrative Example: Relabeling Process and Period Selection

The operation begins with the detection of triangular structures, which are essentially subgraphs comprising three nodes, each intricately connected to the other two. This initial step lays the foundation for a deeper exploration of the network's intricacies. Subsequently, the characteristics of the edges within these detected triangles are rigorously examined. This critical assessment helps to delineate whether the edges hold a positive or negative nature. The outcome of this assessment forms the basis for the subsequent classification.

The classification operation itself is a pivotal stage in our analysis. Based on the nature of the edges within the triangle, we categorize these structures into two primary classes: positive and negative triangles. The implications of this classification are profound, as they shed light on the nature of relationships within the network. Positive triangles, characterized by edges that all bear a positive connotation, signify stable and reinforcing relationship structures. These configurations often represent mutually beneficial associations that contribute to the overall cohesion of the network. Understanding the prevalence and role of positive triangles allows for a nuanced grasp of the network's cooperative dynamics. Conversely, negative triangles encompass at least one edge of a negative nature, denoting potentially unstable or conflicting relationship structures. These configurations merit close attention, as they could signify areas of tension or contradiction within the network. By identifying and analyzing negative triangles, we gain valuable insights into potential areas for intervention or resolution.

We also proceeded to evaluate the prediction power of the models in positive and negative networks, with an expectation of increased accuracy when considering triangle structures. Additionally, signed triangle structures are anticipated to exhibit the highest prediction power. As the network structures incorporate information from both positive and negative networks, they capture a broader range of node behaviors throughout the network process.

Furthermore, we conducted two additional model runs to compare the performance of the signed triangle model when applied to the directed Bitcoin network and the Fraternity network, both with and without directional information. Specifically, we compared the results of the signed triangle model on the original directed networks and modified undirected networks. This comparison allows us to assess the impact of directional information on the prediction power of the signed triangle model.

A.6 Training Process for Bitcoin, CoW, and Fraternity Networks

The training process began with the Bitcoin network dataset, and the last period was initially set as the 17th period. Subsequently, the last period was successively incremented by 1 until reaching the 33rd period. The start period for training was determined as the last period minus 12. Consequently, a total of 17 periods were selected for model training and evaluation purposes. Next, the training process moved to the CoW network dataset, which spanned 51 periods. The training started from the 2nd period, and the last period was initially set as the 6th period. Subsequently, the last period was successively incremented by 1 until reaching the 45th period. Similar to the Bitcoin network, the start period for training was determined as the last period minus 4. This resulted in a selection of 40 periods of data for training and evaluation. Finally, the training process focused on the Fraternity network dataset, which consisted of 15 periods. The training started from the 1st period, and the last period was initially set as the 4th period. Subsequently, the last period was successively decremented by 1 until reaching the 8th period. Similar to the previous datasets, the start period for training was determined as the last period minus 3. This resulted in a selection of 8 periods of data for training and evaluation.

Throughout the training process for all three network datasets, our models underwent extensive simulations. Each model was executed 250 times, with the entire process being repeated 590 times. This rigorous approach was adopted to ensure the robustness and reliability of our research findings. In our study, we utilized various models to analyze network dynamics and predictive capabilities. The simulation of these models involved defining the parameters and variables for each model to capture the unique characteristics and dynamics of the networks under investigation. The models were then run multiple times, with each run utilizing different training data or settings and producing predictions or simulation results. Following each model run, we evaluated its performance metrics, including predictive accuracy and consistency of simulation outcomes. The decision to repeat the model simulations 590 times was driven by several important considerations. When dealing with uncertain or stochastic data in our research, conducting multiple model runs allowed us to address variability.

Each run could employ different random data samples to ensure the consistency and robustness of the results. Repeating the simulations enabled the generation of multiple sets of experimental outcomes, facilitating statistical inference, such as calculating average performance and confidence intervals, which helped us assess the overall model performance more effectively. Additionally, running the models repeatedly provided the opportunity to fine-tune model parameters and settings to identify optimal configurations that enhanced performance. This approach ensured the consistency of model performance across various scenarios, thus guaranteeing the reliability and generalizability of our research findings.

A.7 Evaluation of Model Performance Using PR-AUC

To evaluate model performance, we adopt the Precision-Recall Area Under Curve (PR-AUC) value as the indicator. The PR curve encompasses the true positive rate as the x-axis and the precision as the y-axis. We estimate the BTERGM model based on the temporal network data from $[t-4, t-1]$ and then test the prediction accuracy on the network of time t. As [5] suggest, the PR-AUC value is a better choice than the more common ROC-AUC value when predicting a sparse network. The PR value, on the one hand, focuses on accurately identifying the true positive. On the other hand, the ROC-AUC value puts equal weight on successfully identifying true positives and true negatives. Therefore, modeling networks with many zeros might inflate the prediction power. Identical to the ROC-AUC value, PR-AUC also takes a value from 0 to 1, and the higher number suggests a higher accuracy rate.

Model Name	Baseline	GW-ESP	Single-layer Triangle	Signed Triangle
Variables	(1) Edges, Mutual (Pos.)	(7) Edges, Mutual, GW-ESP (Pos.)	(13) Edges, Mutual, Form, Brk (Pos.)	(19) Edges, Mutual, SForm, SBrk (Pos.)
	(2) Edges, Mutual (Neg.)	(8) Edges, Mutual, GW-ESP (Neg.)	(14) Edges, Mutual, Form, Brk (Neg.)	(20) Edges, Mutual, SForm, SBrk (Neg.)
	(3) Edges, Mutual, SF-Bal, SB-Bal (Pos.)	(9) Edges, Mutual, GW-ESP, SF-Bal,SB-Bal (Pos.)	(15) Edges, Mutual, Form, Brk, SF-Bal, SB-Bal (Pos.)	(21) Edges, Mutual, SForm, SBrk, SF-Bal, SB-Bal (Pos.)
	(4) Edges, Mutual, SF-Bal, SB-Bal (Neg.)	(10) Edges, Mutual, GW-ESP, SF-Bal, SB-Bal (Neg.)	(16) Edges, Mutual, Form, Brk, SF-Bal, SB-Bal (Neg.)	(22) Edges, Mutual, SForm, SBrk, SF-Bal, SB-Bal (Neg.)
	(5) Edges, Mutual, SF-NBal, SB-NBal (Pos.)	(11) Edges, Mutual, GW-ESP, SF-NBal, SB-NBal (Pos.)	(17) Edges, Mutual, Form, Brk, SF-NBal, SB-NBal (Pos.)	(23) Edges, Mutual,SForm, SBrk, SF-NBal, SB-NBal (Pos.)
	(6) Edges, Mutual, SF-NBal, SB-NBal (Neg.)	(12) Edges, Mutual, GW-ESP, SF-NBal, SB-NBal (Neg.)	(18) Edges, Mutual, Form, Brk, SF-NBal, SB-NBal (Neg.)	(24) Edges, Mutual, SForm, SBrk, SF-NBal, SB-NBal (Neg.)

Table 2: Model Types

Model Name	**Network Type**
Signed Triangle (Directed)	Directed Bitcoin Network
Signed Triangle (Undirected)	Modified Undirected Bitcoin Network
Signed Triangle (Directed)	Directed Fraternity Network
Signed Triangle (Undirected)	Modified Undirected Fraternity Network

Table 3:
Comparison of Signed Triangle Model on Directed and Modified Undirected Networks

References

[1] Aref, Samin and Mark C Wilson. 2019. "Balance and frustration in signed networks." *Journal of Complex Networks* 7(2):163–189.

[2] Chen, Ted Hsuan Yun. 2021. "Statistical inference for multilayer networks in political science." *Political Science Research and Methods* 9(2):380–397.

[3] Estrada, Ernesto. 2019. "Rethinking structural balance in signed social networks." *Discrete Applied Mathematics* 268:70–90.

[4] Leifeld, Philip, Skyler J Cranmer and Bruce A Desmarais. 2018. "Temporal exponential random graph models with btergm: Estimation and bootstrap confidence intervals." *Journal of Statistical Software* 83(6).

[5] Thurner, Paul W, Christian S Schmid, Skyler J Cranmer and Göran Kauermann. 2019. "Network interdependencies and the evolution of the international arms trade." *Journal of Conflict Resolution* 63(7):1736–1764.